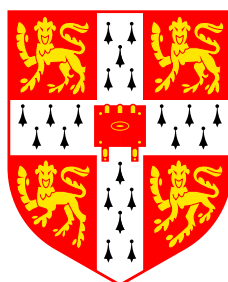


# First Principles Calculation of Nuclear Magnetic Resonance Parameters

A dissertation submitted for the degree of  
*Doctor of Philosophy*  
at the University of Cambridge



Jonathan Robert Yates  
Christ's College, Cambridge

July 2003

# Preface

This dissertation describes work done between October 1999 and July 2003 in the Theory of Condensed Matter group at the Cavendish Laboratory under the supervision of Prof. M.C. Payne.

This dissertation is my own work and contains nothing which is the outcome of work done in collaboration with others, except as specified in the text and Acknowledgements. This dissertation has not been submitted in whole or in part for any degree or diploma at this or any other university.

Jonathan Robert Yates  
Cambridge, July 2003

# Acknowledgements

I have been very fortunate to benefit from the support, enthusiasm and knowledge of numerous people over the last four years. I can only mention a few. Firstly my supervisor, Mike Payne, who provided just the right mix of freedom and guidance.

I am especially grateful to my main collaborators, Chris Pickard and Francesco Mauri. They have both taught me a great many things and this thesis is built upon their previous work. Sian Joyce and Mickael Profeta both helped me with many aspects of this work.

The Theory of Condensed Matter Group has been a supportive home for the last four years. In particular I thank Matt Segall for his encouragement and interest and Michael Rutter for keeping the computers in line!

I have learnt much from my, very patient, experimental collaborators. The porphyrins of Chapter 4 were synthesised and studied by Richard Kowenicki and Nick Bampos of Cambridge University Chemical Laboratory. Kevin Pike and Ray Dupree of the University of Warwick provided me with the spectra of Glutamic Acid for the work of Chapter 5 and taught me about quadrupolar nuclei. I also thank Phuong Ghi and Robin Harris of the University of Durham for many useful discussions.

I would like to thank the members of the Laboratoire de Minéralogie-Cristallographie de Paris for their hospitality during my time in Paris which was funded by a European Union Marie Curie Host Fellowship.

I thank the EPSRC for a research studentship and the Isaac Newton Trust for a Newton Research Student Award. The final year of this work was funded by a Research Fellowship from Corpus Christi College. Computational time was provided by the Cambridge-Cranfield High Performance Computing Facility.

And finally my parents for their support.

## 1.2 Outline of Dissertation

In Chapter 2 we give an overview of first principles quantum mechanical simulation focusing on density functional theory and the plane-wave pseudopotential technique. We show how the projector augmented wave method gives a intuitive approach to pseudopotential theory and provides a natural framework for calculating all-electron properties from a pseudopotential calculation.

In Chapter 3 we present a method for calculating NMR chemical shifts in which the core electrons are represented by so-called “ultrasoft” pseudopotentials. This builds upon previous work which was limited to norm-conserving pseudopotentials. The extension to ultrasoft pseudopotentials is important as it allows us to treat larger, more complex systems. Validation of the method and some technical details of its implementation are also given.

In Chapter 4 we apply first principles techniques to calculate the NMR parameters for a variety of porphyrin systems, a biologically relevant class of organic molecules. We are able to rationalize the chemical shieldings in terms of intense currents which circulate the molecular framework.

In Chapter 5 we address a problem from solid-state NMR. There is little empirical understanding of  $^{17}\text{O}$  NMR and we use first principles techniques to assign the experimental spectra of glutamic acid, an important amino acid. We extend this work to consider several crystal structures of glutamic acid and draw general conclusions about the influence of hydrogen bonding on  $^{17}\text{O}$  NMR parameters.

In Chapter 6 we consider the calculation of chemical shielding parameters for heavy nuclei. We combine the Zeroth Order Regular Approximation (ZORA) to the Dirac equation with the methods outlined in Chapter 3 and show that relativistic effects of the valence electrons are of critical importance. We demonstrate the success of the method with calculations on a range of Selenium and Tellurium containing molecules. In Appendix C we use this formalism to rigorously justify the use of relativistic pseudopotentials in electronic structure calculations.

Finally, in Chapter 7 we outline the directions for future work in this field.

# Chapter 4

## Porphyryns and Ring Currents

### 4.1 Introduction

Porphyryns are a class of compounds intimately connected to the existence of life. They have in common the same structural heart, a tetra-pyrrole macrocycle (Fig. 4.1). It is the aromatic nature of this macrocycle that dominates the chemical and spectral properties of porphyryns. For example it gives rise to the intense colour of porphyryn compounds.

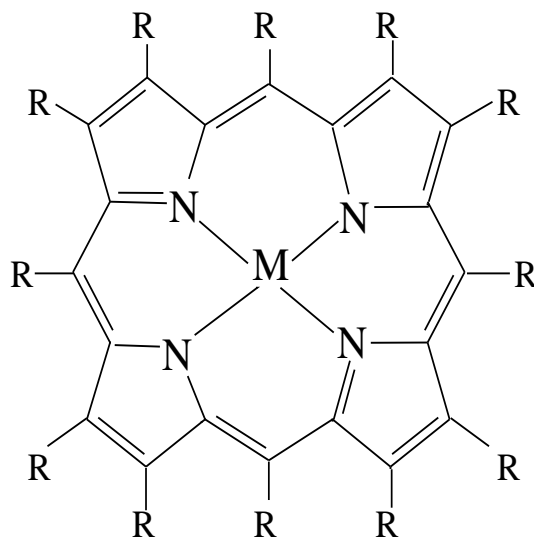


**Figure 4.1:** Porphyrin macrocycle. M is a metal ion, R is a substituent group

The porphyrin macrocycle is able to bind metal ions, which act as centres for biochemical reactions. Small changes to the porphyrin structure lead to a wide diversity of biological function. An iron porphyrin, heme is involved with the transport of oxygen in blood as

well as many of the body's metabolic processes. A magnesium porphyrin, chlorophyll, is responsible for photosynthesis and the characteristic green colour of plants. Vitamin B<sub>12</sub> is a cobalt containing porphyrin. Natural porphyrins such as these are shielded from chemical attack by a surrounding protein casing. For example, the myoglobin complex is composed of a heme active site surrounded by a basket like globin protein. In an aqueous environment the iron(II) active site would quickly become oxidised to iron(III) and be rendered inactive. The protein forms a hydrophobic pocket around the heme enabling it to reversibly bind to oxygen. The protein can also enhance the specific action of the porphyrin by requiring ligands to approach in a particular orientation.

Given the ubiquity of porphyrins in nature, it is unsurprising that much effort has been spent on producing synthetic porphyrins with properties tuned for particular tasks. For example the optical properties of porphyrins have been harnessed for research into solar cells. Synthetic porphyrins can also be used to mimic the enzymatic reaction of natural porphyrins for example, to gain insight into the mechanisms of drug metabolism.

However, synthetic porphyrins do not have the protein casing found in nature. Instead bulky substituent groups must be attached to the porphyrin macrocycle. These have several uses. They increase the solubility of the porphyrin, allowing aqueous reactions. The substituent also stabilises the porphyrin increasing its resistance to chemical attack. Most importantly the substituent groups control the specific action of the porphyrin. Recent work has led to large porphyrin cages, in which the porphyrin is capable of binding, recognition and catalysis [47].

NMR is routinely used in the study of synthetic porphyrins to characterise reaction products. Often the synthesis of a particular compound can involve several stages and take many days. Advance knowledge of the spectral fingerprint of the final product would be very valuable. Prediction of porphyrin chemical shifts is challenging due to the presence of ring currents, intense electronic currents which flow around the aromatic macrocycle [48]. Atoms inside the porphyrin macrocycle experience a shielding effect, those outside are deshielded by the ring current, Fig 4.2. The ring current has its greatest effect on proton shifts giving rise to shifts at both extremes of the shielding scale. Empirical ring current models have been used for many years to predict chemical shifts however their practicality is limited as they must be parametrised for each class of porphyrin compound.

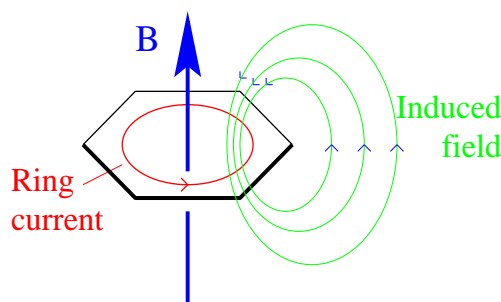


**Figure 4.2:** Schematic Diagram of a ring current

First Principle calculation require no such parameterisation and can thus provide a general and powerful tool.

## 4.2 Validation

We shall consider first the simplest, un-substituted porphyrins. As well as providing a good validation study this will also allow a comparison with larger, more chemically relevant porphyrins. We can thus judge the effects of adding substituent groups. Such small porphyrins are insoluble, however, solid state NMR data is available.

We consider both a zinc and a free-base porphyrin. Free-base porphyrin has no central metal ion, charge neutrality is maintained by two H atom attached to the inner N atoms. Two configurations of the inner H are possible, either a *cis* or *trans* arrangement as shown in Fig. 4.3.

The structure of both configurations was optimised using ultrasoft pseudopotentials with a planewave cut-off energy of 340eV in a  $15\text{\AA}$  cubic supercell. The *trans* configuration was found to be the lower energy structure, in line with a simple viewpoint. The *cis* configuration was 0.30eV higher in energy. This corresponds to a characteristic Boltzmann temperature of 3500K and at room temperature we would expect the population of the *cis* configuration to be less than 1 in  $10^6$ . In later calculations we only consider the *trans* configuration.

At 0K *trans* freebase porphyrin structure has the structure shown in Fig. 4.3, with two inequivalent N sites. The effects of temperature on this structure have been widely studied experimentally [49]. At low temperatures two distinct peaks are observed in the  $^{15}\text{N}$  spectra, at room temperatures there is just one peak. The protons exchange at a rate

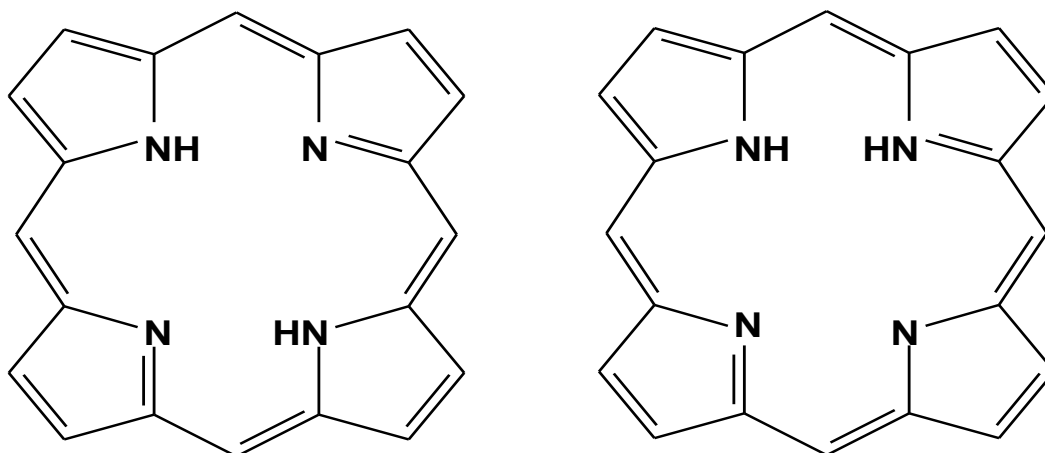


**Figure 4.3:** Trans (left) and Cis (right) Configurations of Free-base porphyrin

much shorter than the NMR time scale.

### 4.2.1 Calculations

The chemical shieldings for free-base and Zinc porphyrin were calculated using the methods outlined in Chapter 3 and [36] for norm-conserving pseudopotentials. The pseudopotentials used were of the Troullier and Martins [16] form. A planewave cut-off energy of 70Ryd (1000eV) was used which gives  $^{13}\text{C}$  shieldings converged to within 1ppm and  $^1\text{H}$  shieldings to within 0.1ppm. In the case of free-base porphyrin we present results averaged over the two tautomeric configurations related by fast proton exchange.

From our *ab-initio* calculations we obtain absolute chemical shieldings. Experimentally chemical shifts are measured relative to a given standard reference compound (for  $^{13}\text{C}$  and  $^1\text{H}$  this is Tetra-Methyl Silane, TMS). To compare our absolute value to experiment we set the average *ab-initio* shieldings for  $^{13}\text{C}$  and  $^1\text{H}$  in pyrrole equal to their experimentally measured chemical shifts.

### 4.2.2 Results

### 4.2.3 Discussion

The calculated  $^{13}\text{C}$  shifts for both molecules agree well with the experimental values. The maximum error is 4ppm (C5). It is pleasing to note that the relative differences are ex-



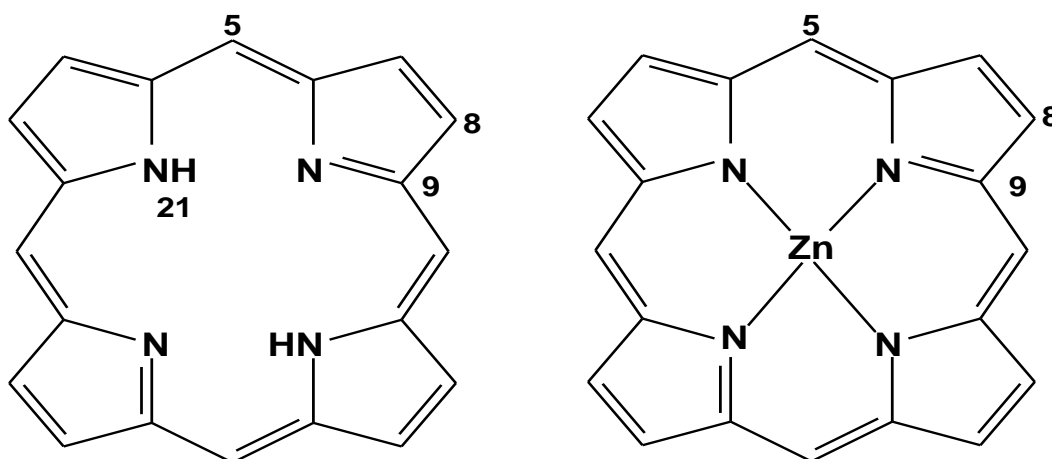


**Figure 4.4:** Free-base and Zinc Porphyrin. Distinct NMR sites labelled according to IUPAC scheme

Atom	Free-base Porphyrin		Zinc Porphyrin	
	Calc(ppm)	Expt	Calc(ppm)	Expt
C5	102	106.03	102	106.50
C8	130	133.56	130	133.95
C9	145	147.16	149	151.84
H5	10.79	10.43	10.72	10.34
H8	10.24	9.57	10.26	9.54
H21	-4.03	-3.91	-	-

**Table 4.1:** Calculated and experimental chemical shifts (relative to TMS). Experimental data from *The Porphyrin Handbook* (2000) Ed. Kadish and refs therein

tremely well reproduced, in particular the 4ppm difference between the C9 shift in freebase and Zinc Porphyrin. The maximum error in the proton shifts is 0.7ppm for H8. However the shift of the inner proton, H23, which is at the extreme shielding end of the shift scale, is well reproduced (an error of 0.1ppm). The effects of the ring current on the proton shifts is dramatic, with a 15ppm difference between inside and outside the macrocycle.

### 4.3 Large porphyrins

Having gained confidence in our techniques from the study of small porphyrins we now turn our attention to larger systems, typical of the compounds used in everyday re-

search. We study 10,20-Diphenyl-3,7,13,17-Tetraethyl-2,8,12,18-Tetramethyl Porphyrin

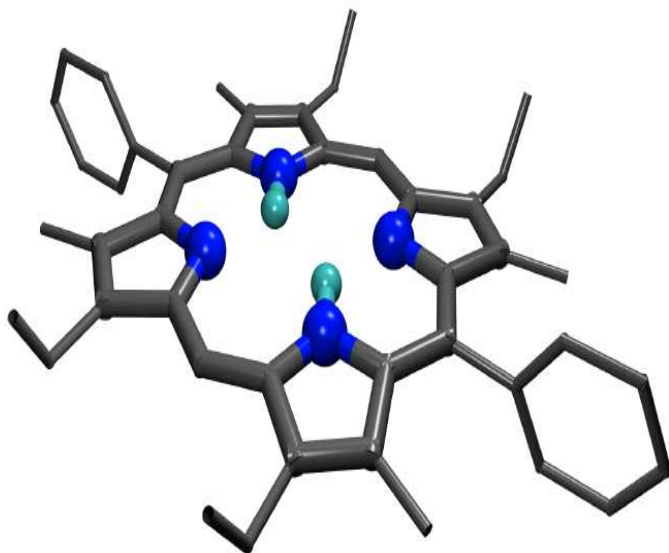


**Figure 4.5:** Large Porphyrin

(DPTETM) which has phenyl groups at two of the meso positions and ethyl and methyl groups attached to each pyrrole ring, Fig.4.5. This compound was synthesised and its NMR spectra measured by Richard Kowenicki and Dr. Nick Bampos of Cambridge University Chemical Laboratory.

Obtaining the ground state geometry poses several challenges. First, for the free-base structure, there is again the question of the *cis trans* configuration of the inner hydrogens. We find that although the energy difference between the two configuration is smaller than in the unsubstituted porphyrin (0.2eV) the *cis* conformation still forms a very small fraction of the total population. More seriously, at room temperature the substituent groups will be free to rotate, this rotation will be fast on the NMR timescale. The shift of a given atom will be proportional to the average field it experiences. Under such rotations atoms will move above and below the macrocycle plane, at each position the magnetic field due to the ring current will be different. In principle a molecular dynamics simulation could be performed with the NMR shift calculated as an ensemble average, however this would be computationally very expensive. The global minimum energy structure will have the greatest contribution and other structures will contribute according to their Boltzmann

weight. The lowest energy structure was found to be as Fig. 4.5 with ethyl groups pointing out of the plane of the porphyrin macrocycle <sup>1</sup>. Structures with one or more ethyl groups aligned in the plane of the porphyrin macrocycle are local minima. We found the energy of the structure with one ethyl group in the plane of the macrocycle to be 0.5eV above the ground state structure, structures with more than one such ethyl group have still higher energies. As a result of these calculations it is clear that the structure with all of the ethyl groups pointing out of the macrocycle plane will give the dominant contribution to the measured chemical shifts. NMR Chemical shieldings were calculated and the results averaged over identical sites.

### 4.3.1 Results

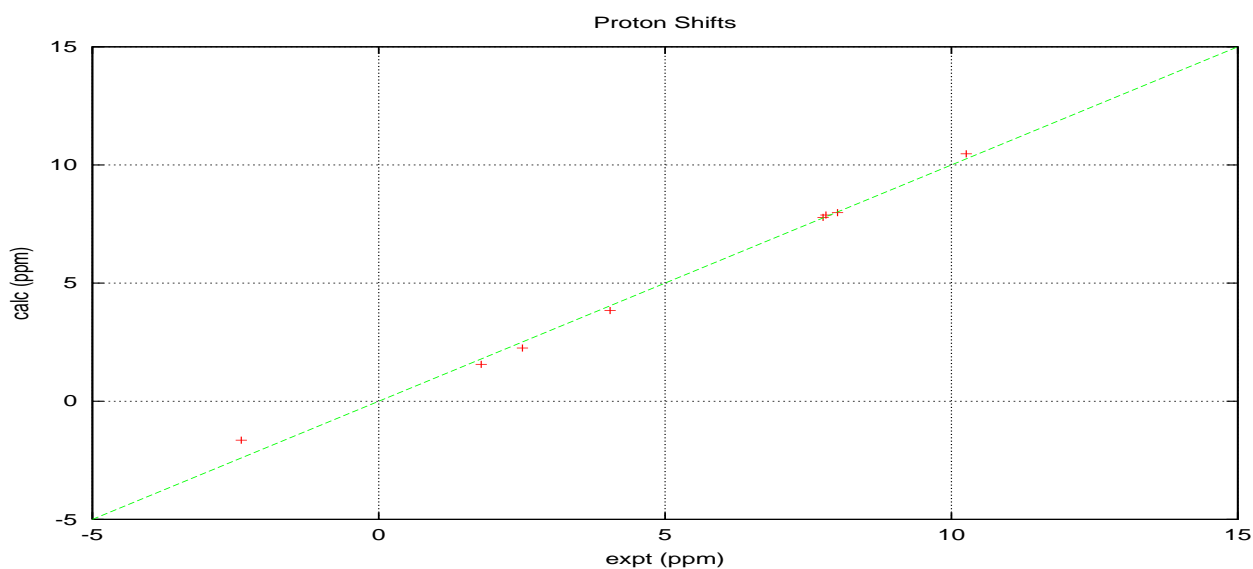


**Figure 4.6:** Ab-Initio vs Experimental Proton shifts for DPTETM-Porphyrin

### 4.3.2 Discussion

The agreement between calculated and experimental proton shifts, Fig. 4.6, is excellent. All peaks have their correct assignment with a mean error of 0.2ppm . There is similarly good agreement between calculated and experimental <sup>13</sup>C shifts, Fig. 4.7, with a mean

---

<sup>1</sup>this can occur in several ways; eg two ethyls pointing above the plane and two below. All these permutations were found to be very close in energy and gave identical NMR parameters

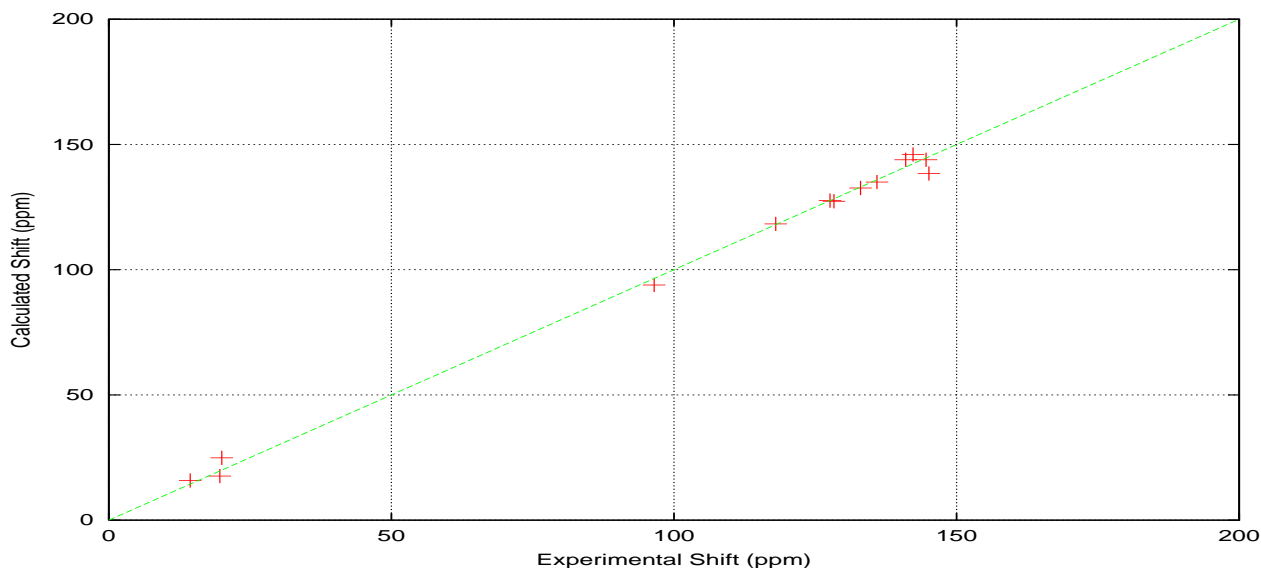


**Figure 4.7:** Ab-Initio vs Experimental  $^{13}\text{C}$  shifts DPTETM-Porphyrin

error of 4ppm. All peaks have their correct assignment except for one peak which is part of a small cluster with shifts around 145ppm.

## 4.4 Ring Currents

The existence of ring currents was first proposed by Linus Pauling over sixty years ago [50] in order to explain the diamagnetic anisotropy of benzene.

“... the assumption that the  $2p_z$  electrons are free to move under the influence of the impressed field from carbon atom to adjacent carbon atom.” [50]

Since then most of the vast literature devoted to ring currents has focused on the study of benzene, the archetypal aromatic compound. However the effect of the benzene ring current on the proton shifts is fairly small ( $\sigma_{benzene}=7.27\text{ppm}$ ,  $\sigma_{ethene}=5.25\text{ppm}$ ). As we have seen in Secs. (4.2 and 4.3) ring currents have a dramatic influence on the proton shifts in porphyrins. Unlike simple mono-cyclic compounds such as benzene, porphyrins have several aromatic pathways which can contribute to the total ring current. To the best of our knowledge no *ab-initio* current density maps have been published for porphyrin. As we calculate the chemical shielding from the induced current we obtain these plots at no extra cost. Although it is not possible to measure current density directly from experiment

the excellent agreement between our calculated shifts and experiment gives us confidence in the validity of our *ab-initio* current maps.

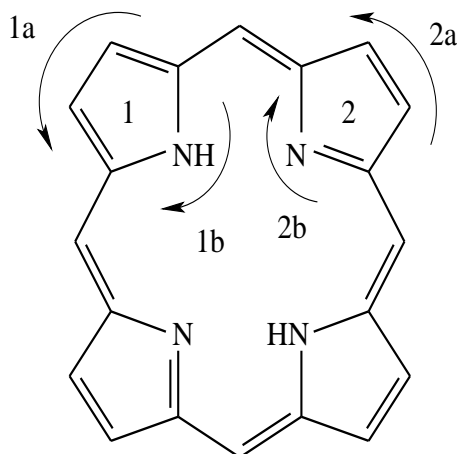


**Figure 4.8:** Possible Ring Current Pathways in Porphyrin

Figs. 4.9 and 4.10 show the computed current density in planes parallel to the porphyrin macrocycle due to a magnetic field perpendicular to the macrocycle. For clarity results are shown for the unsubstituted porphyrin of Sec. 4.2 but the results for DPTETM-porphyrin are qualitatively similar. In the plane of the macrocycle itself the main feature of the plots are large paramagnetic circulations about the Carbon and Nitrogen atoms. One can also clearly see the diamagnetic flow of current outside the perimeter of the macrocycle, correspondingly there is a paramagnetic flow inside the perimeter. These flows are present in any cyclic molecule (eg non-aromatic hexane) and are unrelated to the ring current as they do not correspond to a net flux of current around the macrocycle. From the plots of current density above the macrocycle the strong diamagnetic ring current can clearly be seen. In the case of freebase porphyrin the current has different flow patterns around the two distinct pyrrole groups, labelled 1 and 2 in Fig. 4.8. In the group without an inner H (2) the flow is predominately over the C-N-C bonds (pathway 2b) whilst in the group with an inner H (1) the current appears to flow roughly equally around the two possible routes (1a and 1b).

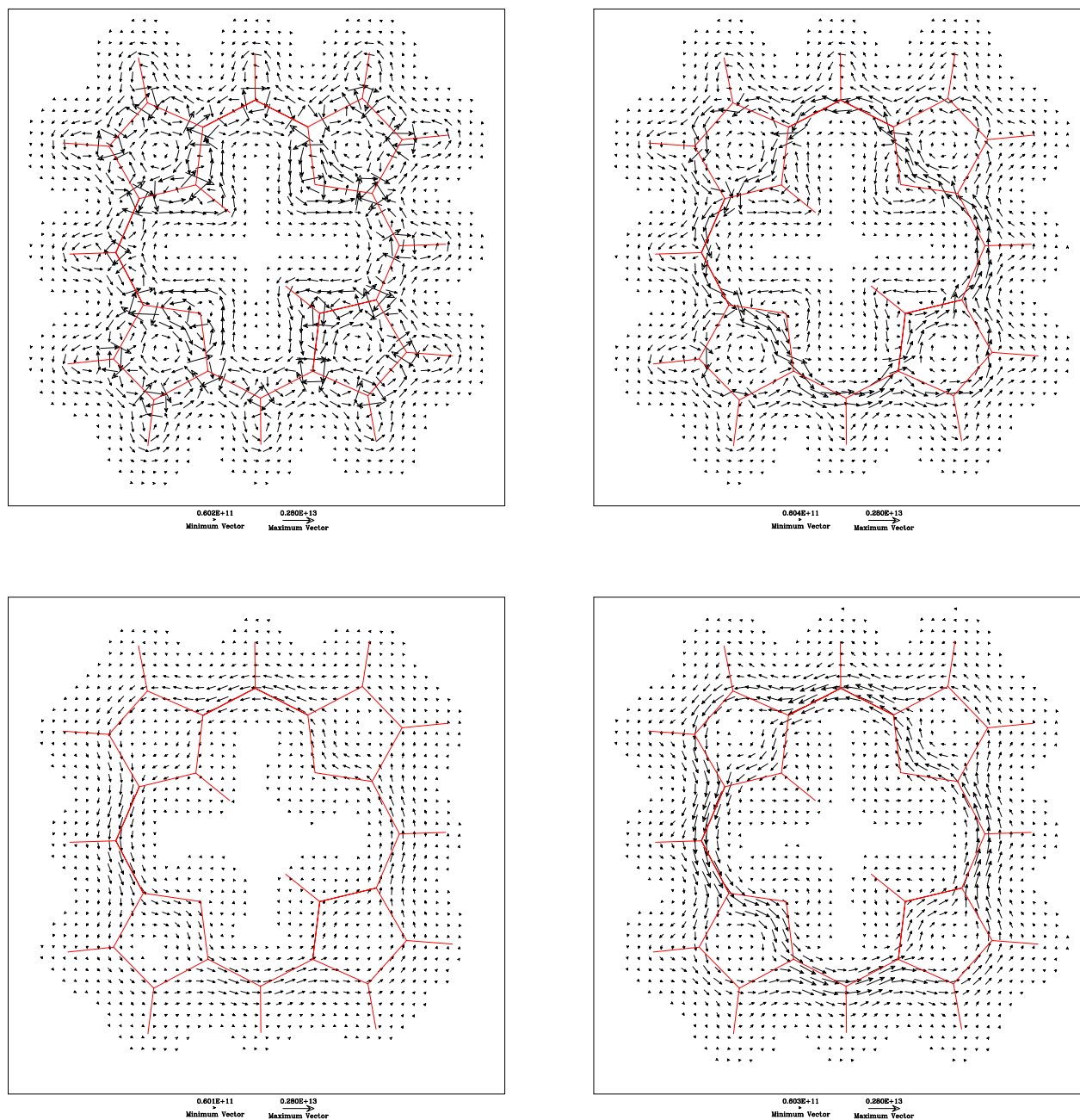


**Figure 4.9:** Current flow in porphyrin. Height above molecular plane clockwise from top left: 0.0, 0.53, 1.05, 1.58 (Bohr). For each graph the scaling of the vectors is the same, Minimum:  $0.6 \times 10^{11} nAT^{-1} Bohr^{-2}$  Maximum:  $0.3 \times 10^{13} nAT^{-1} Bohr^{-2}$

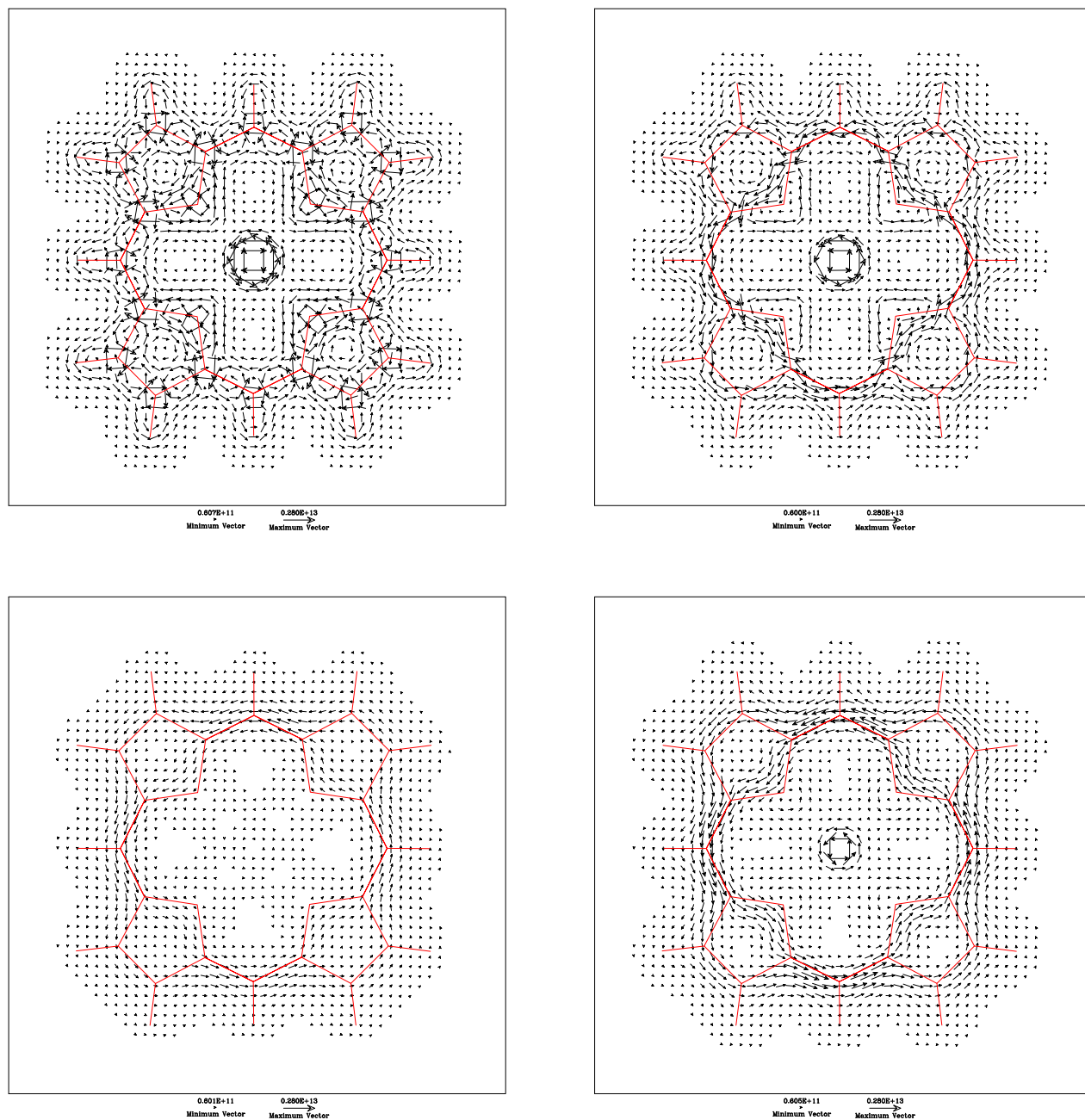


**Figure 4.10:** Current flow in Zinc porphyrin. Height above molecular plane clockwise from top left: 0.0, 0.53, 1.05, 1.58 (Bohr). The scaling of the vectors is as Fig. 4.9

In order to examine more closely the flow of current around the porphyrin macrocycle we calculated the current flux at several points. This involved integrating the current density flowing in the direction of a bond across a plane perpendicular to the bond. The results for porphyrin are shown in Fig. 4.11, for comparison the total ring current of a variety of aromatic molecules is summarised in Table 4.2.

Molecules	Ring Current ( $nAT^{-1}$ )
Benzene	11.5
Pyrrrole	11.9
unsub-freebase porphyrin	25.8
DPTETM-freebase porphyrin	24.0

**Table 4.2:** Current Flux in Various Aromatic Compounds

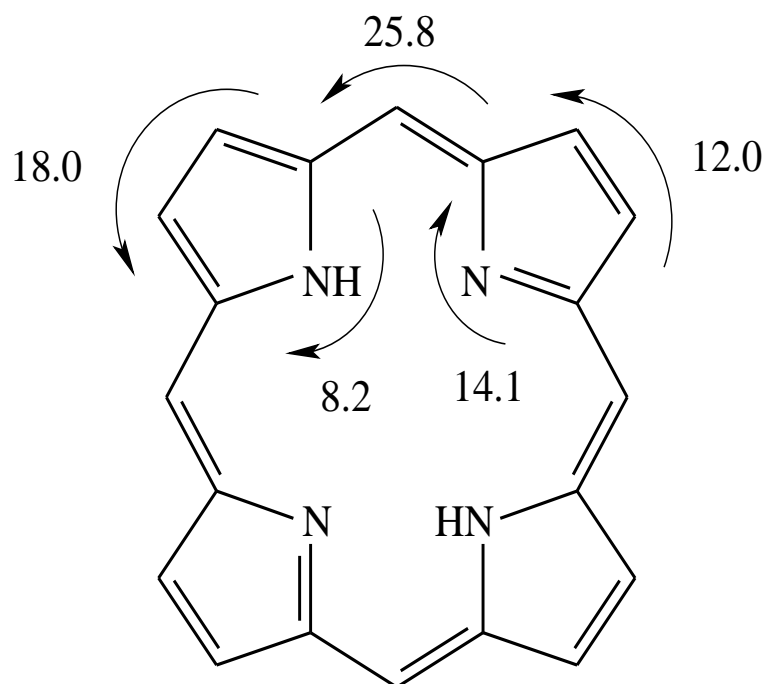


**Figure 4.11:** Current Flux in Porphyrin,  $nAT^{-1}$ . The error on these values is  $\pm 0.2nAT^{-1}$ .

From Table 4.2 it is clear that the macrocycle ring current in both porphyrins is much larger than in either pyrrole or benzene. The current flux in DPTETM-freebase porphyrin is slightly less than in the unsubstituted porphyrin. This is reflected in the shifts on the inner protons, which are less shielded in DPTETM-freebase porphyrin ( $\sigma = -2.4$  ppm



compared to  $\sigma=-3.91$  in the unsubstituted porphyrin). From Fig 4.11 and the current plots in Fig 4.9 it can be seen that the flow of current is a superposition of all possible pathways. The calculated flux shown in Fig 4.11 must be interpreted carefully. The flux along the inner pathways (shown as 1a and 2a in Fig 4.8) will be decreased by the non-ring current paramagnetic flow inside the macrocycle, the flux along the outer pathways (1b and 2b) will be similarly increased due to the outer non-ring current diamagnetic flow (these currents of course give no net contribution to the ring current). The plots in Fig 4.9 support the assertion [51] that the main ring current pathway is a combination of the  $18\pi$  electron inner cross and two aromatic pyrrole rings (labelled 1 and 3), Fig. 4.12. This is in contrast to the popular description of the porphyrin skeleton as a bridged annulene derivative [52].

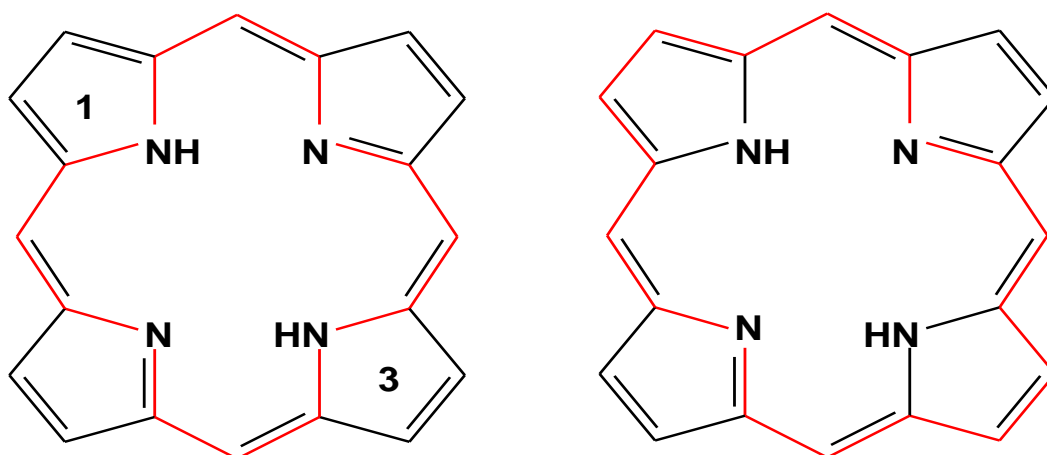


**Figure 4.12:** Possible ring current pathways in porphyrin. Left,  $18\pi$  inner cross with two aromatic pyrrole groups. Right, bridged annulene structure

## 4.5 Conclusions

We have seen that *ab-initio* calculations are able to accurately predict chemical shifts in large porphyrin compounds. This should prove a useful tool to aid experimentalists. To provide some context; the synthesis of the TETMDP porphyrin took about one week. The *ab-initio* calculation of its NMR spectra took about a day (using computational resources available in most UK universities). *Ab-initio* calculations provide a deeper rationalisation of the experimental spectra. Hopefully this information can turn help to improve the treatment of ring currents in empirical models of NMR chemical shifts.

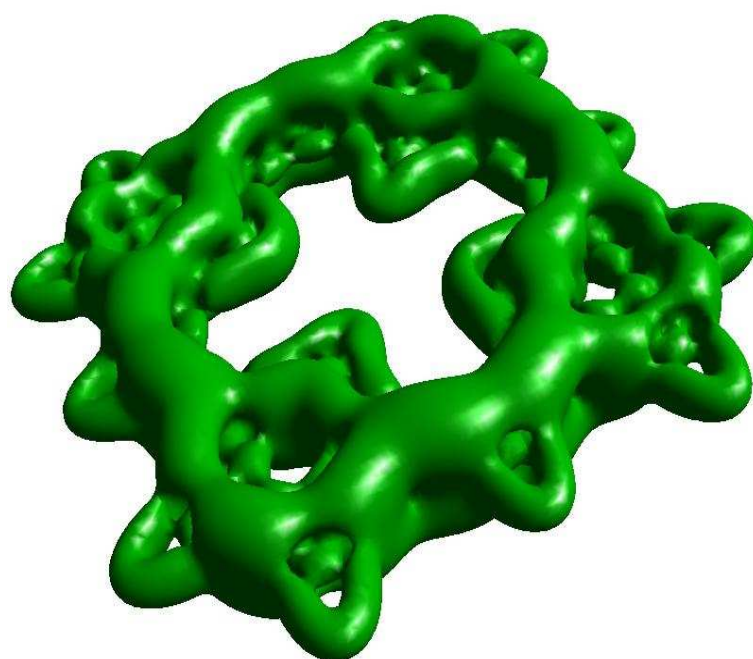


**Figure 4.13:** Current Flux Isosurface in Porphyrin